Plasticity of Hippocampus Following Perinatal Asphyxia: Effects on Postnatal Apoptosis and Neurogenesis

P. Morales,[1] J.L. Fiedler,[2] S. Andrés,[2] C. Berrios,[2] P. Huaiquín,[1] D. Bustamante,[1] S. Cardenas,[1] E. Parra,[3] and M. Herrera-Marschitz[1]*

[1]Programme of Molecular and Clinical Pharmacology, ICBM, Medical Faculty, University of Chile, Santiago, Chile
[2]Department of Biochemistry and Molecular Biology, Chemical and Pharmaceutical Sciences Faculty, University of Chile, Santiago, Chile
[3]University of Tarapaca, Arica, Chile

Asphyxia during delivery produces long-term deficits in brain development, including hippocampus. We investigated hippocampal plasticity after perinatal asphyxia, measuring postnatal apoptosis and neurogenesis. Asphyxia was performed by immersing rat fetuses with uterine horns removed from ready-to-deliver rats into a water bath for 20 min. Caesarean-delivered pups were used as controls. The animals were euthanized 1 week or 1 month after birth. Apoptotic nuclear morphology and DNA breaks were assessed by Hoechst and TUNEL assays. Neurogenesis was estimated by bromodeoxyuridine/MAP-2 immunocytochemitry, and the levels and expression of proteins related to apoptosis and cell proliferation were measured by Western blots and in situ hybridization, respectively. There was an increase of apoptosis in CA1, CA3, and dentate gyrus (DG) and cell proliferation and neurogenesis in CA1, DG, and hilus regions of hippocampus 1 week after asphyxia. The increase of apoptosis in CA3 and cell proliferation in the suprapyramidal band of DG was still observed 1 month following asphyxia. There was an increase of BAD, BCL-2, ERK2, and bFGF levels in whole hippocampus and bFGF expression in CA1 and CA2 and hilus at P7 and P30. There was a concomitant decrease of phosphorylated-BAD (Ser112) levels. The increase of BAD levels supports the idea of delayed cell death after perinatal asphyxia, whereas the increases of BCL-2, ERK2, and bFGF levels suggest the activation of neuroprotective and repair pathways. In conclusion, perinatal asphyxia induces short- and long-term regionally specific plastic changes, including delayed cell death and neurogenesis, involving pro- and antiapoptotic as well as mitogenic proteins, favoring hippocampal functional recovery. ○

Key words: neonatal; hypoxia; cell death; cell proliferation; rat

Asphyxia is a major cause of death and neurological injury in newborns, frequently associated with difficult or prolonged delivery (Vannucci and Hagberg, 2004). There is clinical and experimental evidence indicating that the neurocircuitries of the hippocampus are vulnerable for perinatal asphyxia (van Erp et al., 2002; see Harry and d'Hellencourt, 2003). Delayed cell death has been observed days after global (Kirino et al., 1984; Dell'Anna et al., 1997) or focal (Nakano et al., 1990) hypoxia/ischemia, involving CA1 (Kirino et al., 1984), CA3 (Nakajima et al., 2000), and dentate gyrus (DG; Wang et al., 1999a) regions, with features suggesting apoptosis (Nakajima et al., 2000; Northington et al., 2001). The extent of cell loss produced by hypoxia-ischemia depends on the severity of the insult as well as on the stage of brain development when the insult occurs (Vannucci and Hagberg, 2004). Indeed, there is evidence showing that the neonatal brain is more vulnerable to oxidative stress than the mature brain, probably because of low antioxidant capability (Aspberg and Tottmar, 1992), leading to accumulation of hydrogen peroxide in particularly vulnerable brain regions, including the hippocampus (Lafemina et al., 2006).

Apoptosis is triggered by the activation of endogenous proteases (caspases), resulting in cytoskeletal disruption, cell shrinkage, and membrane blebbing. The nucleus undergoes chromatin condensation and nuclear DNA degradation resulting from endonuclease activation (see Yuan and Yankner, 2000). The BCL-2 protein family encodes specific proteins that regulate apoptosis under

Contract grant sponsor: FONDECYT; Contract grant numbers: 1080447, 11070192, 1080489, 1060774.

*Correspondence to: Prof. Mario Herrera-Marschitz, MD Sci, PhD, Programme of Molecular and Clinical Pharmacology, ICBM, Medical Faculty, University of Chile, P.O. Box 70000, Santiago 7, Chile.
E-mail: mh-marschitz@med.uchile.cl

different physiological and pathological conditions (see Davies, 1995). BCL-2 and BCL-X_L promote survival (Howard et al., 2002), whereas BAX, BID, and BCL-X_S accelerate apoptotic cell death, promoting mitochondrial cytochrome c release, activating intrinsic apoptotic pathways (see Cory et al., 2003). The BCL-X_L/BCL-2-associated death promoter (BAD) acts as a proapoptotic protein (Yang et al., 1995). Apoptotic stimuli, including anoxia, induce dephosphorylation of cytosolic BAD (Wang et al., 1999b), which is then dissociated from the 14-3-3 protein chaperone and translocated to the mitochondria, where it binds to BCL-2 and BCL-X_L, promoting mitochondria cytochrome c release (Yang et al., 1995; Zha et al., 1996). Otherwise, BAD is maintained in the cytosol, phosphorylated by the activation of the ERK and/or AKT pathways, bound to the 14-3-3 protein, exerting an antiapoptotic effect (Zha et al., 1996; Jin et al., 2002).

Multiple cell death mediators are activated by neonatal hypoxia-ischemia injury, including various members of the BCL-2 (Chen et al., 1996; Ness et al., 2006), death receptor (Graham et al., 2004), and caspase (Cheng et al., 1998; see Golan and Huleihel, 2006) protein families. After neonatal hypoxia-ischemic conditions, there is an increase in the number of immunoreactive cells for proapoptotic proteins, BAX and caspase 3, correlating with an increase of apoptosis in the hippocampus (Ferrer et al., 1997; Daval et al., 2004). In agreement, BAD gene-disrupted mice exhibit protection against neonatal hypoxia-ischemia (Ness et al., 2006). In an adult rat model of global ischemia, it has been shown that BAD/BCL-X_L binding is increased in CA1 and DG regions (Abe et al., 2004).

During the reoxygenating phase, there are some mechanisms for limiting cell death but also for promoting plastic changes, including neurogenesis and neuritogenesis, required for functional recovery. Several neurotrophins, such as basic fibroblast growth factor (bFGF; Andersson et al., 1995), brain-derived neurotrophic factor (BDNF; Scheepens et al., 2003a), and neuronal growth factor (NGF; Scheepens et al., 2003a), are upregulated following asphyxia, probably for preventing cell death (Cheng et al., 1997; Han and Holtzman, 2000). Indeed, there is evidence that bFGF expression is increased by hypoxia-ischemic injuries, promoting cell survival and neurogenesis (Takami et al., 1992; Andersson et al., 1995; Ganat et al., 2002), in agreement with evidence showing that bFGF controls neural proliferation and cell migration during development but also during the postnatal period, including adulthood (see Dono, 2003). Hence, postnatal neurogenesis can be a mechanism to replace cell loss and to repair altered neurocircuitry, perhaps using mechanisms similar to those required for neuritogenesis. In agreement, neurogenesis is increased in juvenile (Scheepens et al., 2003b; Daval et al., 2004) and adult (Yagita et al., 2001; Yoshimura et al., 2001) rat hippocampus, including DG (Morales et al., 2005; Lichtenwalner and Parent, 2006) and CA1–CA3 (Nakatomi et al., 2002; Daval et al., 2004) regions following hypoxia-ischemia.

Therefore, we have investigated the consequences of perinatal asphyxia on hippocampal plasticity, using a noninvasive experimental model largely mimicking the main features of asphyxia occurring at birth (Bjelke et al., 1991; Andersson et al., 1992; Herrera-Marschitz et al., 1993; see Weitzdoerfer et al., 2004). We have focused on the effects observed 1 week (P7) and 1 month (P30) after birth, measuring 1) apoptosis (by Hoechst and TUNEL assays), 2) neurogenesis [by bromodeoxyuridine (BrdU)/MAP-2 immunocytochemitry], and 3) levels and expression of proteins related to apoptosis and mitogenesis (by Western blots and in situ hybridization). We focus on the effects observed at P7 and P30, because P7 is a period when granular layers of the hippocampus are established (Bayer, 1982) and there is a beginning of intensive synaptogenesis (Amaral and Dent, 1981), and P30 is a period when the neurocircuitry of the hippocampus of the rat has already achieved mature features (Amaral and Witter, 1995).

MATERIALS AND METHODS

Perinatal Asphyxia

Pregnant Wistar rats (UChA, bred at a local colony) within the last day of gestation (G22) were euthanized by neck dislocation and hysterectomized. One or two pups were immediately removed and used as caesarean-delivered controls (CS), and the uterine horns containing the remaining fetuses were immersed in a water bath at 37°C for 20 min (AS), a period associated with a 50% decrease in survival (Herrera-Marschitz et al., 1993; Bustamante et al., 2007). After asphyxia, the uterine horns were incised, and the pups were removed and stimulated to breathe. After a 60-min observation period, the pups were given to surrogate dams for nursing, pending further experiments. At P7 and P30, the rats were used for 1) immunocytochemistry, 2) immunoblotting, and/or 3) in situ hybridization studies.

For BrdU analysis, the rats were treated with BrdU (100 mg/kg, i.p.; Sigma, St. Louis, MO) dissolved in 0.1 M phosphate-buffered saline (PBS; four doses with 4-hr intervals over a 12-hr period), and killed 4 hr after the last dose of BrdU.

Tissue Fixation

Rats were deeply anesthetized with chloral hydrate (400 mg/kg i.p.) and perfused intracardially with 100 ml of 0.1 M PBS (pH 7.4), followed by 200 ml formalin solution [4% paraformaldehyde (PF); Sigma; in 0.1 M PBS, pH 7.4]. The brain was removed from the skull, postfixed in a formalin solution overnight, and immersed in 30% sucrose in 0.1 M of PBS at 4°C for 2–3 days; then embedded in cryomatrix (Thermo Electron Corp, Pittsburgh, PA) and stored at −70°C. Coronal sections (20 μm thick) were sliced from the frozen fixed brains and processed between Bregma −4.52 and −2.56 (Paxinos and Watson, 1986) for immunocytochemistry.

Immunocytochemistry

Cellular proliferation was labelled with an antibody against the mitotic marker BrdU (Megabase, Lincoln, NE) and neuronal phenotype with an antibody against MAP-2

(Sigma). The tissue was first treated for MAP-2. The stored slices were postfixed in methanol 100% (J.T. Backer, Paris, KY) for 30 min; rinsed three times; and preincubated in 0.1 M PBS, 0.1% Triton, and 5% normal goat serum (NGS; Jackson Immunoresearch, West Grove, PA) for 1 hr. A mouse monoclonal antibody against MAP-2, immunospecific for all forms of mature and immature neurons (Sigma; dilution 1:2,000, 5% NGS and 0.1% Triton in 0.1 M PBS), was applied overnight at 4°C. After extensive washings, sections were incubated in a Tyramide Amplification Kit No. 3 (TSA; Molecular Probes, Eugene, OR), according to the instructions of the supplier. After that, the tissue was postfixed in 4% PF for 15 min at 4°C and washed extensively to preserve the integrity of the MAP-2 staining according to Kobayashi et al. (2006).

For BrdU, the slices were treated with 2 N HCl for 30 min at 37°C for DNA denaturation; extensively washed in 0.1 M PBS; and incubated in 0.1 M PBS, 5% NGS, and 0.1% Triton for 1 hr at room temperature. A rabbit polyclonal antibody against BrdU (dilution 1:4,000, 5% NGS and 0.1% Triton in 0.1 M PBS; Megabase) was applied overnight at 4°C. After extensive washings, sections were incubated in the TSA Kit No. 12. The sections were washed again, coverslipped with DAKO fluorescent mounting medium (DAKO, Carpinteria, CA), and examined under the field of an epifluorescence and a confocal microscope. Selected slices were counterstained with propidium iodide (PI; 500 nM for 5 min; Sigma) for confirming the nuclear labelling.

Cell Quantification, Optical Disector, and Confocal Microscopy

Stereological quantification was conducted as previously described (Morales et al., 2005). Confocal microscopy was performed by using a Zeiss LSM410 confocal laser scanning microscope with a ×633 (1.4 N.A.) oil-immersion objective lens. Hippocampal MAP-2- and/or BrdU-immunoreactive (IR) cells were counted by an investigator blinded to the protocol treatment, using the optical disector technique described in detail by Gundersen et al. (1988). Briefly, MAP-2- or BrdU-IR cells were counted as they came into focus while scanning through the section. The disector height (h) was set at 10 μm, and nuclei within the first 3 μm of the section were not counted. Also, we discarded all the nuclei that intersected the left and the bottom sides of the frame. For each section, six unbiased counting frames were sampled in a systematically random fashion inside the area of hippocampal subfields. The area of disector (a_{dis}) was set at 4.5×10^4 μm^2. The area (a) of hippocampal subfields was measured in Image J 1.32 software. The total number of MAP-2- or BrdU-positive cells in each hippocampal region was then estimated as: $N = \Sigma Q^- \cdot t/h \cdot a/a_{dis}$, where Q^- is the total number of counted MAP-2- or BrdU-positive cells in each hippocampal region, t is the average slice thickness, a is the area of hippocampal region, a_{dis} is the area of disector, and h is the dissector height. Cells were considered doubly labelled when MAP-2 and BrdU overlapped at four levels through a section (z-step 1 μm).

Apoptotic Morphology

Coronal sections were stained with Hoechst 33342 (bisbenzimide; 2.5 μg/μl; Sigma) and mounted with a fluorescent mounting medium (DAKO). Hoechst 33342 is used for investigating nuclear morphology, revealing chromatin condensation during apoptosis, which is detected as an intensively bright blue staining. Apoptotic nuclei were identified by using the criteria proposed by Greiner et al. (2001). Briefly, at least one of the following criteria had to be fulfilled to count for apoptotic cells: 1) tightly condensed nuclear material, 2) darkly stained spherical or clumped nuclear material, and 3) fragmented nuclei. An average of the number of apoptotic cells was calculated from five slices/animal (one slice of 20 μm every 100 μm), inspected at ×100, and expressed as means ± SEM.

DNA Fragmentation

Coronal sections were processed according to the TUNEL-based detection kit NeuroTACS (R&D Systems, Minneapolis, MN). Briefly, coronal slices from each animal were washed in 0.1 M PBS for 10 min at room temperature, incubated with a Neuropore solution (R&D Systems) for 25 min at room temperature, and washed twice in DNAase-free water for 2 min or in the presence of DNAase as a positive control. The samples were then immersed in an H_2O_2 quenching solution for 5 min, washed in PBS, and incubated in terminal deoxynucleotidyl transferase (TdT) labelling buffer for 5 min at room temperature. Afterward, a reaction buffer containing biotinylated dNTP and TdT was applied for 90 min at 37°C in a humidity chamber. As a negative control, a set of sections was incubated in the absence of TdT. The reaction was stopped with TdT stop buffer, and the slices were washed twice with PBS and incubated with streptavidin-HRP solution for 10 min. After PBS rinsing, the slides were immersed in the diaminobenzidine (DAB) solution for 4–10 min, washed with PBS, counterstained with Neuro TACS Blue for nuclear labelling (R&D Systems), dehydrated in a graded ethanol series, and mounted with Entellan (Merck, Darmstadt, Germany). An average of the number of dark brown DAB-stained nucleus (TUNEL positive) was calculated from five slices/animal (one slice of 20 μm every 100 μm), inspected at ×100, and expressed as means ± SEM.

In Situ Hybridization

The in situ hybridization was conducted with an oligonucleotide probe complementary to bFGF mRNA (732pb-763pb access No. NM_019305.1; Shimasaki et al., 1988), labelled with digoxigenin oligonucleotide 3′-OH tailing kit (Roche Molecular Biochemicals, Mannheim, Germany). The labelled oligonucleotide was ethanol precipitated and resuspended in DEPC-treated water.

The hybridization was performed as previously described by Cárdenas et al. (2002). In brief, coronal brain slices were washed in 0.1 M PBS, permeated with 0.001% proteinase K (molecular biology grade; Merck), and then treated with 0.25% acetic anhydride in 0.1 M triethanolamine. After dehydration in increasing concentrations of ethanol, the slices were delipidated in chloroform for 10 min, rinsed in ethanol, and

air dried. Hybridization was carried out with 50 pmol/ml bFGF digoxigenin oligonucleotide in the presence of 4× SSC solution, 50% formamide, 1% Denhart's solution, 50 μg/ml sheared salmon sperm DNA, 10% dextran sulfate, and 125 μg/ml tRNA (37°C for 16 hr in a humidity chamber). The hybridization was stopped with 2× SSC solution, and the slides were immersed in successive washing solutions of 4× SSC for 10 min, 2× SSC (3 times 15 min each). A final wash (2× SSC) was done at 37°C for 15 min. To visualize the digoxigenin-hybridized probe, the slides were incubated for 2 hr in a solution of 0.1 M maleic acid, 150 mM NaCl, pH 7.4 (buffer 1), in the presence of 0.03% Triton X-100, 3% fetal calf serum, antidigoxigenin Fab fragments conjugated with alkaline phosphatase (dilution 1:500; Roche), and 1% blocking reagent for nucleic acid hybridization (Roche). After quickly rinsing in buffer 1, sections were incubated in 100 mM NaCl, 50 mM $MgCl_2$, 100 mM Tris (pH 9.5) in the presence of the alkaline phosphatase substrate 5-bromo-4-chloro-3-indolyl phosphate/nitroblue tetrazolium (BCIP/NBT) and 0.024% levamizole for 16 hr at room temperature. The reaction was stopped by a 30-min wash in 10 mM Tris, 1 mM EDTA, pH 8.0. Controls for specific hybridization were made with an antisense digoxigenin oligonucleotide in the presence of 5 nmol/ml unlabeled probe.

Semiquantitative Analysis of the Hybridization Signal

For the semiquantitative analysis, densitometric measurements from each hippocampal subfield were analyzed in UN-SCAN-IT software (Silk Scientific, Orem, UT). A gray scale was used for measuring the intensity of the signals (pixels) observed in the hippocampal regions; i.e., the darker the staining the higher optical density, and the lighter staining the lower optical density. The hybridization signal in the stratum radiatum was considered as background and was subtracted from the optical density values obtained in the hippocampal cell layers. Data are expressed as optical density (pixels), and for each animal the value represents the average of measurements made from four or five brain sections.

Western Blotting Analysis

In a separate, but similarly treated, series of animals, the hippocampus was dissected and homogenized with a glass-glass homogenizer in 5 vol 10 mM HEPES, pH 7.9, 1.5 mM $MgCl_2$, 10 mM KCl, 0.1 mM EGTA, 0.1 mM EDTA. 0.5 mM DTT, 0.1 mM Na_3VO_4, 100 μg/ml PMSF, 2 μg/ml leupeptin, 2 μg/ml aprotinin, and 0.05% Triton X-100 according to Greiner et al. (2001) and Andrés et al. (2006). After centrifugation at 10,000*g* for 15 min, the supernatant was collected and the protein content determined according to Bradford (1976). 50 μg of protein extract was resolved on a 12% SDS-polyacrylamide gel (PAGE; 100 V) and blotted onto a 0.45-μm nitrocellulose membrane (1 hr, 95 V). The equality of protein loading in the wells was confirmed by Ponceau red (Sigma) staining. For ERK1/2, bFGF, CREB, and β-actin determination, the membranes were treated with a PBS cocktail containing 0.1% Tween-20 (PBST) and 3% (w/v) nonfat dry milk at room temperature for 1 hr. For BAD and BCL-2 determination, the membranes were treated with a Tris-buffered saline (TBS) containing 0.1% Tween-20 (TBST) and 1% (w/v) nonfat dry milk at room temperature for 1 hr.

For evaluation of mitogenic protein levels (bFGF, ERK1, and ERK2), the membranes were incubated with mouse monoclonal bFGF (dilution 1:250; Upstate, Charlottesville, VA) or rabbit polyclonal antibodies phospho-ERK1/2, phospho-ERK1/2 (P-ERK1/2; Thr202/204; dilution 1:3,000; Cell Signalling, Beverly MA), total ERK1/2 (dilution 1:3,000; Santa Cruz Biotechnology, Santa Cruz, CA), total CREB (dilution 1:1,000; Cell Signalling), phospho-CREB (P-CREB; Ser133; dilution 1:1,000; Upstate), or β-actin (dilution 1:5,000; Sigma), in 3% nonfat dry milk-0.1% T-PBS.

The levels of BAD and BCL-2 were measured as previously described (Greiner et al., 2001; Andrés et al., 2006). For phospho-BAD (P-BAD; Ser112) and total BAD, the membranes were incubated with rabbit polyclonal antibody (dilution 1:500; Cell Signalling). For BCL-2, the membranes were incubated with a mouse monoclonal antibody (dilution 1:100; Santa Cruz Biotechnology) in 1% nonfat dry milk diluted in TBS. The membranes were incubated overnight with the primary antibody, then washed and incubated with a peroxidase-conjugated secondary antibody for 2 hr. After additional washes, the membranes were incubated with an enhanced chemiluminescent substrate, according to the instructions of the manufacturer (Perkin Elmer Life Sciences, Boston, MA) and exposed to X-ray film (MR-1; Eastman-Kodak, Rochester, NY). The intensity of the bands was determined and analyzed in UN-SCAN-IT software, and the results were expressed as a ratio to the β-actin. Also, ratios for P-CREB/total CREB, P-ERK/total ERK, and P-BAD/total BAD were determined. All data were normalized to the controls.

Statistical Analysis

The data were obtained from at least six independent experiments (each experiment representing a different litter) using four to six male rats from each experimental group. Values are expressed as the mean ± SEM throughout the study. Multiple (nonparametric) comparisons were analyzed with Kruskal-Wallis's ANOVA (H) and/or Mann-Whitney test (GraphPad Prism 4.00). $P < 0.05$ was used as a limit for statistical significance.

The experimental protocol was approved by a Local Committee for Ethics for Experiments With Laboratory Animals at the Medical Faculty, University of Chile (CBA No. 0136, FMUCH) and by an ad hoc National Commission of the Chilean Council for Science and Technology Research (CONICYT), endorsing the Principles of laboratory animal care (NIH; No. 86-23; revised 1985).

RESULTS

Perinatal Asphyxia Increases Apoptosis in Hippocampus

The hippocampus of CS (control) and AS (asphyxia-exposed) animals was examined for apoptotic morphology after nuclear Hoechst staining and for DNA fragmentation with the TUNEL assay. Figure 1 shows photomicrographs of nuclei labelled with Hoechst in the

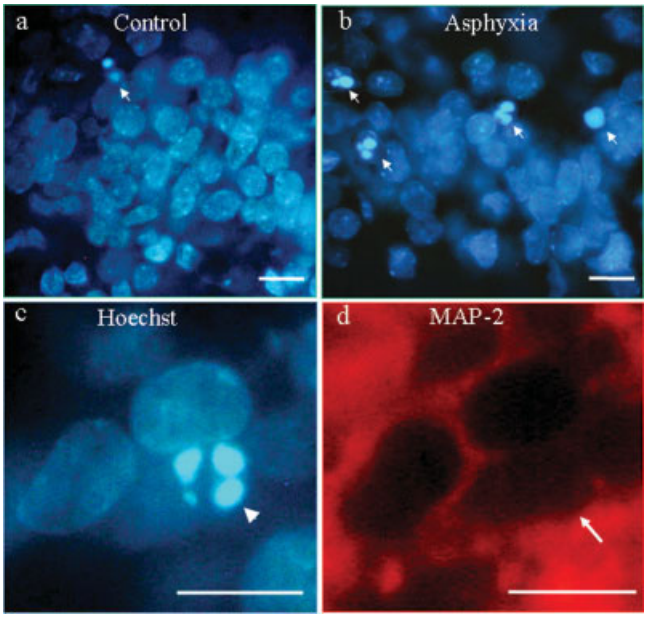

Fig. 1. **a–d:** Fluorescent photomicrographs showing Hoechst-labelled nuclei (blue) and cases of chromatin condensation (bright blue; arrowheads), illustrating apoptotic cell morphology, in suprapyramidal band of control (a) and asphyxia-exposed (b–d) rats at P7. A case showing a chromatin fragmented nucleus (arrowhead; c) was doubly stained with an antibody against MAP-2 (red; arrow; d), indicating a neuronal phenotype. Observe that MAP-2 labels cytoplasm only, surrounding the unstained nuclei. Scale bars = 20 μm.

suprapyramidal band (granular cells) of DG of CS (Fig. 1a) and AS (Fig. 1b–d) rats, depicting nuclei with apoptotic morphology (Fig. 1, arrowheads). Double staining (Hoechst/MAP-2) revealed that approximately 95% of cells with apoptotic morphology were positive for a neuronal phenotype (cf. Fig. 1c vs. d). Figure 2 shows the stereological quantitative analysis of apoptotic nuclei labelled by the Hoechst staining of control (n = 6) and asphyxia-exposed (n = 6) rats at P7 and P30. At P7, a significant increase of the number of apoptotic nuclei was observed in CA3 (>2-fold) and DG (supra- and infrapyramidal bands; >2-fold) of AS compared with CS animals (Fig. 2A). That increase was still observed at P30, but only in the CA3 region (Fig. 2B).

A similar result was observed with the TUNEL assay, showing an increase of apoptotic nuclei in CA1 (∼1.5-fold), CA3 (∼2-fold), and supra- and infrapyramidal (∼1.5-fold) bands of the DG of AS (n = 4) vs. CS (n = 4) animals compared at P7 (Fig. 3). Figure 3 shows photomicrographs illustrating TUNEL-positive nuclei (brown; counterstained with Neuro TACS Blue) in suprapyramidal band at P7 of CS (Fig. 3a) and AS (Fig. 3b) animals.

Perinatal Asphyxia Increases Pro- and Antiapoptotic Protein Levels in Hippocampus

The effect of perinatal asphyxia on the expression of pro- and antiapoptotic proteins, BAD and BCL-2,

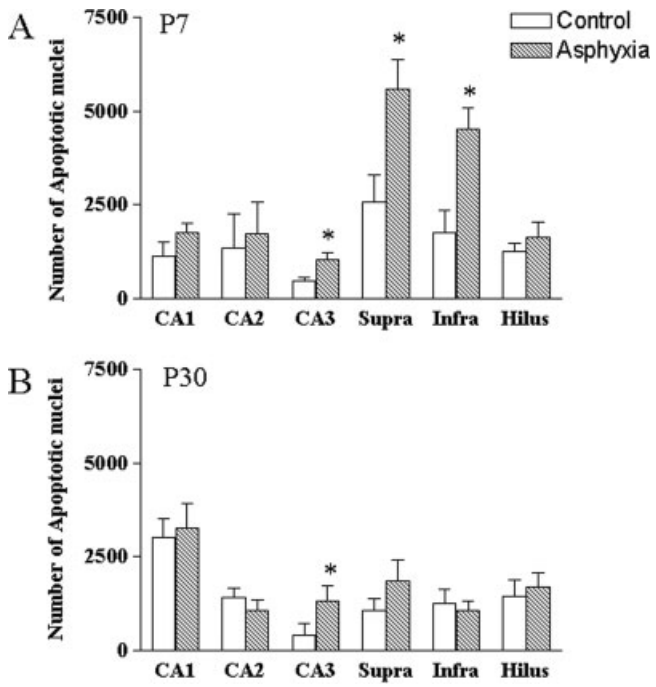

Fig. 2. Quantification of apoptotic nuclei in hippocampus of control (n = 6, open bars) and asphyxia-exposed (n = 6, hatched bars) rats at P7 (**A**) and at P30 (**B**). At P7, there was a significant increase in the number of apoptotic nuclei in CA3 (>2-fold) and DG (supra- and infrapyramidal bands; >2-fold) of asphyxia-exposed compared with control rats. This effect was still observed in CA3 at P30. Data are means ± SEM. $\star P < 0.05$ (Mann-Whitney test).

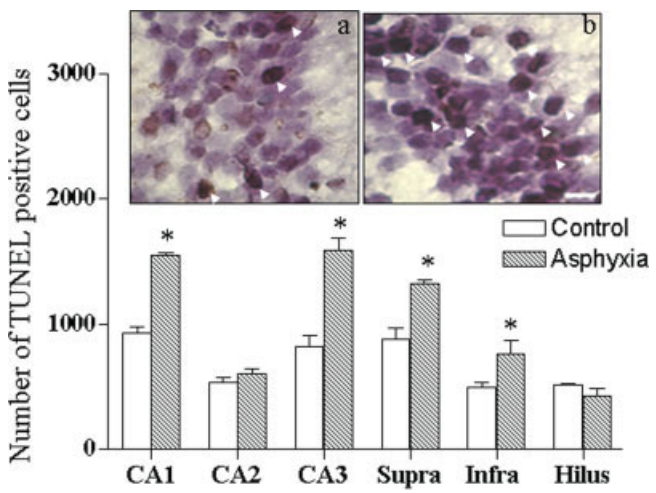

Fig. 3. Quantification of the number of TUNEL-positive nuclei in hippocampus of control (n = 4, open bars) and asphyxia-exposed (n = 4, hatched bars) rats at P7. There was a significant increase in the number of TUNEL-positive nuclei in CA1 (∼1.5-fold), CA3 (∼2-fold), and DG (∼1.5-fold; supra- and infrapyramidal bands) of asphyxia-exposed compared with control rats. Data are means ± SEM. $\star P < 0.05$ (Mann-Whitney test). Photomicrographs illustrate TUNEL-positive (brown; arrowheads) and Neuro-TACS blue (violet)-stained nuclei in the suprapyramidal band at P7 in control (**a**) and asphyxia-exposed (**b**) rats. Scale bar = 20 μm.

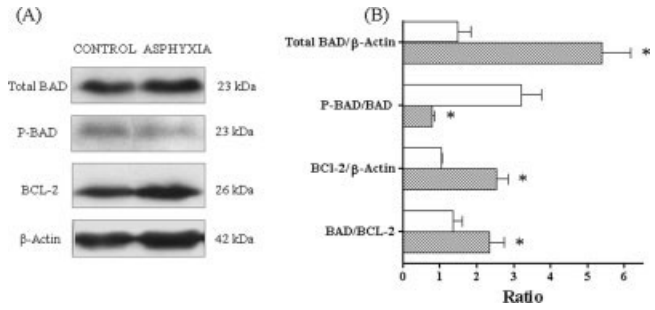

Fig. 4. **A:** Immunoblots from hippocampal extracts of control and asphyxia-exposed rats at P7. Samples (50 μg protein/lane) were resolved by SDS-PAGE, followed by immunoblotting with BCL-2, BAD, phospho-BAD, and β-actin antibodies as described in Materials and Methods. In **B**, the densitometric analysis of the intensity of protein bands of control (n = 4–5, open bars) and asphyxia-exposed (n = 4–5, hatched bars) rats is shown. There was a significant increase of total BAD/β-actin (>3-fold), BCL-2/β-actin (>2-fold), and BAD/BCL-2 (∼2-fold) ratio in samples of asphyxia-exposed compared with control rats. The P-BAD/total BAD ratio was instead decreased (by 70%) in samples of asphyxia-exposed animals. Data are means ± SEM. $\star P < 0.05$ (Mann-Whitney test).

respectively, was investigated with immuno-Western blots. Figure 4A shows representative immunoblots for total BAD, P-BAD (Ser112), and BCL-2 levels of hippocampal extracts obtained from CS and AS animals at P7. The densitometric analysis (Fig. 4B) revealed that there was an increase (>3-fold) of the BAD/β-actin ratio of AS (n = 4–5) compared with CS (n = 4–5) animals. The ratio P-BAD/total BAD was decreased (by ∼70%), whereas the ratio BCL-2/β-actin was increased (>2-fold), following perinatal asphyxia. Also, the ratio BAD/BCL-2 was increased in AS (∼2-fold) compared with CS animals.

Perinatal Asphyxia Increases Cell Proliferation in Hippocampus

To assay cell proliferation, the rats were injected with BrdU (100 mg/kg, i.p.) at P6 and P29, starting 24 hr before the brain was removed, and treated for BrdU immunoreactivity (the last dose of BrdU was administered 4 hr before death). As shown in Figure 5, the stereological analysis revealed that there was a significant increase in the number of BrdU-positive nuclei in DG (supra- and infrapyramidal bands; ∼1.5-fold) and hilus (∼1.5-fold) of AS (n = 6) compared with CS (n = 6) animals. That increase was still observed (∼2-fold) 1 month following asphyxia (P30, n = 6 for each condition), but only in the suprapyramidal band of DG. Figure 5 shows photomicrographs illustrating BrdU-positive nuclei in the suprapyramidal band of DG of CS (Fig. 5a) and AS (Fig. 5b) animals.

There was also a significant increase in CA1 (∼2-fold) at P7, but the total amount of BrdU-positive cells observed in that region was significantly lower than that in DG regions (as an average, there were ∼2,500 BrdU-positive cells in CA1 vs. ∼25,000 BrdU-positive cells in DG regions). At P30, no differences between groups were observed in the number of BrdU-positive cells in the CA1 region.

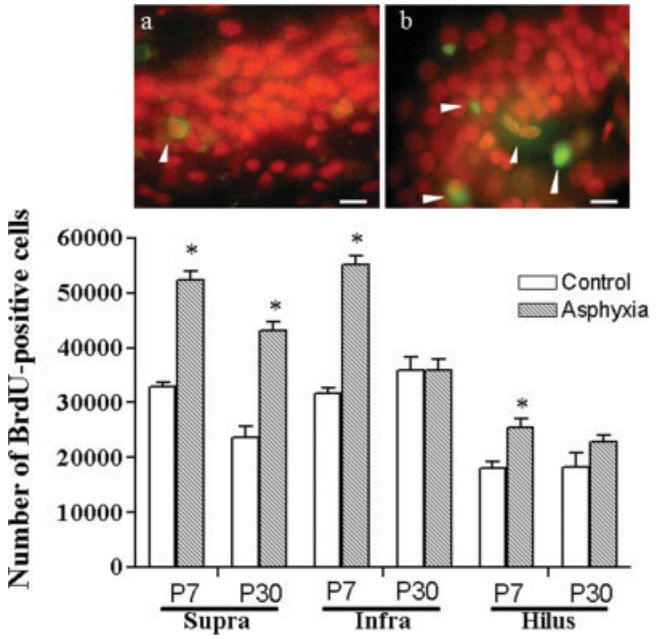

Fig. 5. Quantification of BrdU-positive cells observed in hippocampus of control (n = 6, open bars) and asphyxia-exposed (n = 6, hatched bars) rats at P7 and P30. There was a significant increase of BrdU positive cells in DG (supra- and infrapyramidal bands) of asphyxia-exposed (hatched bars) compared with control (open bars) rats. At P7, there was an increase of BrdU-positive cells in CA1 region (∼2-fold) following asphyxia, but the total amount of BrdU-positive cells observed in that region was significantly lower than in DG (as an average, there were ∼2,500 BrdU-positive cells in CA1 vs. ∼25,000 BrdU-positive cells in DG regions of control animals). At P30, no differences between groups were observed in the number of BrdU-positive cells in the CA1 region. Photomicrographs illustrate BrdU-positive (green; arrowheads) and PI (red)-stained nuclei in suprapyramidal band at P7 in control (**a**) and asphyxia-exposed (**b**) rats. Data are means ± SEM. $\star P < 0.005$ (Mann-Whitney test). Scale bars = 20 μm.

Perinatal Asphyxia Increases Neurogenesis in Hippocampus

The phenotype of BrdU-positive cells was evaluated by double immunostaining with an antibody against MAP-2. In the suprapyramidal band, 40% and 38% of BrdU-positive cells were also positive for MAP-2 in CS and AS animals, respectively. In the infrapyramidal band, the percentage was 42% for both conditions. In the hilus, the percentage was 30% and 20%, for CS and AS animals, respectively. No double-labelled cells were observed in any of the regions of the corni ammonis of CS animals, but 10% of BrdU cells in CA1 of AS animals were also positive for MAP-2.

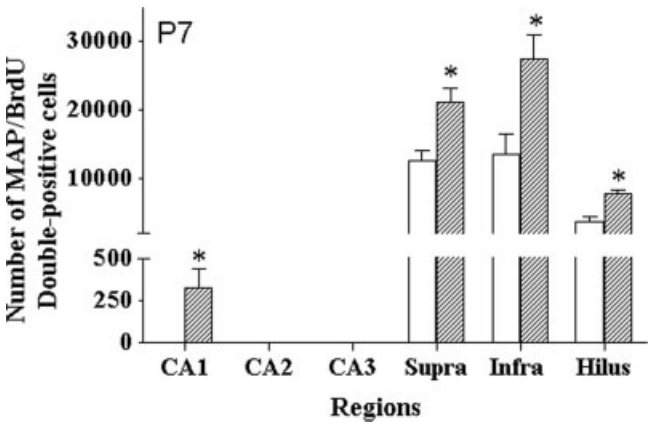

Fig. 6. Quantification of BrdU/MAP-2 double-labelled cells observed in hippocampus of control (n = 6, open bars) and asphyxia-exposed (n = 6, hatched bars) rats at P7. There was a significant increase of BrdU/MAP-2 double-labelled cells in CA1 (~300 cells compared with 0 cells in the controls), DG (supra- and infrapyramidal bands; ~2-fold), and hilus (1.5-fold) of asphyxia-exposed compared with control rats. No BrdU/MAP-2 double-labelled cells were observed in any of the regions of the cornu ammonis of control rats. Data are means ± SEM. $\star P < 0.005$ (Mann-Whitney test).

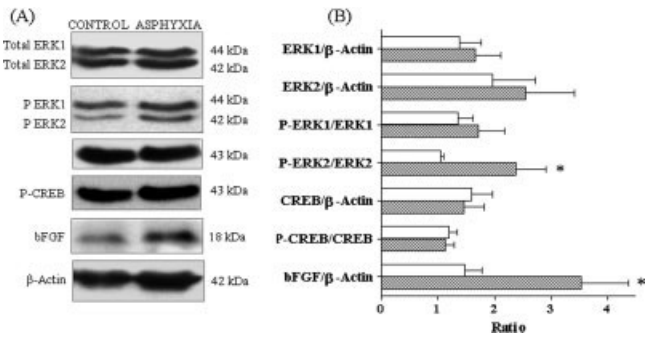

Fig. 7. **A:** Immunoblots from hippocampal extracts of control and asphyxia-exposed rats at P7. Samples (50 μg protein/lane) were resolved by SDS-PAGE, followed by immunoblotting with ERK1/2, P-ERK1/2, CREB, P-CREB, bFGF, and β-actin antibodies as described in Materials and Methods. In **B**, the densitometric analysis of the intensity of the protein bands of control (n = 5, open bars) and asphyxia-exposed (n = 5, hatched bars) rats is shown. There was a significant increase of P-ERK2/ERK2 (>2-fold) and bFGF/β-actin (>2-fold) ratio in samples of asphyxia-exposed compared with control rats. Data are means ± SEM. $\star P < 0.05$ (Mann-Whitney test).

In comparison with CS (n = 6), double-stained cells were increased in DG (supra- and infrapyramidal bands; ~2-fold) and hilus (1.5-fold) of AS (n = 6) animals. Some few double-stained cells (~300 double-stained cells) were observed in CA1 of AS but never in CS animals (Fig. 6). Hoechst staining indicated no evidence of cell death among BrdU/MAP-2-positive cells in any of the regions of the hippocampus.

Perinatal Asphyxia Increases the Levels of ERK2 and bFGF in Hippocampus

Proteins involved in cell proliferation and differentiation were measured with immuno-Western blots in hippocampal extracts from control (n = 5) and asphyxia-exposed (n = 5) rats at P7. Figure 7A shows representative blots for ERK1/2, CREB, and bFGF. The densitometric analyses revealed an increase in the ratio P-ERK2/total ERK2 (>2-fold) following perinatal asphyxia, but not in P-ERK1/total ERK1, CREB/β-actin, or P-CREB/total CREB. However, the ratio bFGF/β-actin was increased (>2-fold) in AS compared with CS animals (see Fig. 7B).

Figure 8A shows in situ hybridization photomicrographs illustrating the increase of bFGF expression in hippocampus of AS (Fig. 8b,d) vs. CS (Fig. 8a,c) animals at P7 (Fig. 8a,b; n = 5, for each condition) and at P30 (Fig. 8c,d; n = 5, for each condition). Figure 8B shows the densitometric analysis of bFGF mRNA at P7, revealing an increase in CA1 (~2-fold) and CA2 (~2-fold) regions and hilus (~2-fold) of AS compared with CS animals. Figure 8C shows the effect at P30, finding an increase in CA1–CA2 (~1.5-fold) and hilus (~3-fold). The level of bFGF protein measured at P7 with immuno-Western blot was also increased (>3-fold) in AS compared with CS (see Fig. 8B, inset).

DISCUSSION

In this study, we have investigated the effects of perinatal asphyxia on cell death, neurogenesis, and differential expression of related genes in the hippocampal formation of rats. There was an increase of apoptosis in CA1, CA3, and DG regions of hippocampus 1 week (P7) after severe perinatal asphyxia, persisting in CA3 at P30. In parallel, there was an increase of cell proliferation in CA1, DG, and hilus at P7 and in the suprapyramidal band of DG at P30. Double staining revealed neurogenesis in CA1, DG, and hilus at P7. BAD, BCL-2, phosphorylated ERK2, and bFGF levels were increased in whole hippocampus at P7 as well as the expression of bFGF in CA1, CA2, and hilus at P7 and P30. P-BAD levels were, however, decreased in whole hippocampus.

As assessed by Hoechst labelling, cell death was observed in control and asphyxia-exposed animals, exhibiting the characteristic hallmarks of apoptosis, including condensation, chromatin clumping, and fragmentation into spherical apoptotic bodies (Lipton, 1999; Yuan and Yankner, 2000). In control animals, the range of dying cells was 500–3,000 in all regions of the hippocampus at P7, in agreement with previous reports indicating that delayed cell death occurs as a mechanism of postnatal development, for further sculpting the CNS (see Oppenheinm, 1991). After perinatal asphyxia, the range of dying cells was 1,200–5,000, significantly increased in pyramidal CA3 and supra- and infrapyramidal bands of DG. At P30, an asphyxia-related increase of apoptotic-like dying cells was observed only in the CA3 region, although apoptotic-like dying cells were observed throughout the hippocampus, with the highest level occurring within the CA1 region of both control

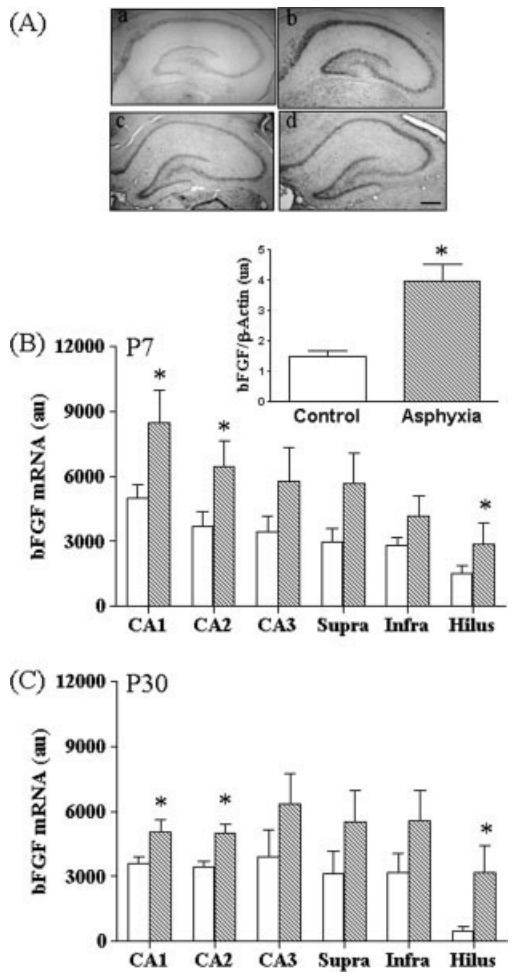

Fig. 8. **A:** Photomicrographs illustrating the expression of bFGF in hippocampus of control (a,c) and asphyxia-exposed (b,d) rats at P7 (a,b, upper panel) and P30 (c,d, lower panel). Densitometric analysis of bFGF mRNA in hippocampus of control (n = 5, open bars) and asphyxia-exposed (n = 5, hatched bars) rats at P7 (**B**) and P30 (**C**). There was a significant increase of bFGF expression in CA1, CA2 (~1.5-fold), and hilus (>2-fold) of asphyxia-exposed compared with control rats at both P7 and P30. Data are means ± SEM. $\star P < 0.05$ (Mann-Whitney test). Scale bar = 200 μm.

(2,000–4,400 dying cells) and asphyxia-exposed (1,400–4,400 dying cells) animals. Perhaps this observation has to be considered when discussing the particular vulnerability of the CA1 region (see Pulsinelli, 1988). Cell death displayed a neuronal phenotype, as shown by MAP-2/Hoechst double labelling, but no dying cells were observed among newly generated cells (BrdU/MAP-2/Hoechst), suggesting that perinatal asphyxia mainly affected nonproliferating cells.

Apoptosis was confirmed by the TUNEL technique, showing a significant increase of TUNEL-positive cells in CA3 and supra- and infrapyramidal bands following perinatal asphyxia at P7. An increase of cell death after asphyxia was also observed in CA1 but reaching a significant level only when evaluated by the TUNEL technique, although a trend for an elevated apoptosis was also observed when labelling with Hoechst at P7.

The expression of proteins involved in the regulation of the apoptotic cascade was analyzed to characterize further the delayed cell death observed after perinatal asphyxia. Mitochondrial membrane permeability has been suggested as a critical factor that activates the apoptotic cascade. Under apoptosis-induced conditions, including hypoxia-ischemia, the mitochondrial membrane increases its permeability, leading to the release of cytochrome c and other proapoptotic factors, such as AIF (Zhu et al., 2003, 2006), Smac/Diablo (Matsumori et al., 2005), and Endo-G (Li et al., 2001). The release of cytochrome c to the cytoplasm causes caspase-3 activation (Daval et al., 2004; Chen et al., 2005). Caspase-3 immunoreactivity has been observed to be elevated 3 days after hypoxia, but that elevation has been shown to be transient (Pourie et al., 2006).

Mitochondrial membrane permeability is regulated by proapoptotic (BCL-X_S, tBID, BAX, BAD) and antiapoptotic (BCL-2, BCL-X_L) members of the BCL-2 protein family (see Cory et al., 2003), which can form homo- and/or heterodimers in the mitochondrial membrane (Yang et al., 1995). Indeed, it has been shown that the expression of BAX and BCL-2 genes is increased in CA1, CA3, and DG following hypoxic-ischemic insults (Chen et al., 1998; Daval et al., 2004). BAD promotes apoptosis through its heterodimerization with the antiapoptotic proteins BCL-2 and/or BCL-X_L (Yang et al., 1995), leading to leakage of mitochondrial proapoptotic factors (Tan et al., 2000). BAD is regulated through selective phosphorylation by several protein kinases, via the AKT and the mitogen-activated protein kinases MEK/ERK pathways (Jin et al., 2002). BAD phosphorylation, at Ser112 and/or Ser136 (Zhu et al., 2002; Hirai et al., 2004), creates binding sites for the chaperone 14-3-3, retaining BAD in the cytoplasm, preventing the heterodimerization with BCL-2 and/or BCL-X_L in the mitochondrial membrane (Zha et al., 1996). BAD phosphorylation at Ser155 also inhibits its death-promoting activity by interfering the binding to BCL-X_L (Tan et al., 2000).

In this study, BAD was increased by perinatal asphyxia, explaining perhaps the apoptosis observed in CA1, CA3, and DG regions. The increase of BAD could be due to enhanced gene expression, decreased protein degradation, and/or other metabolic changes involving phosphorylation/dephosphorylation mechanisms. The enhanced expression of BAD is perhaps a signal for a dangerous condition menacing the integrity of the genome. Otherwise, as shown here, a concomitant decrease of P-BAD (Ser112) could imply a decreased BAD phosphorylation, or an increased phosphatase-dependent dephosphorylation. In agreement, it has been reported that hypoxia-ischemia triggers BAD dephosphorylation by calcineurin (Wang et al., 1999b). In adult gerbils, cerebral ischemia promotes BAD translocation to mitochondria in CA1 but not in the DG region of hippocampus (Dluzniewska et al., 2005). It

was shown that Raf-1, a member of the ERK signalling pathway, was instead decreased in CA1 (Dluzniewska et al., 2005). Furthermore, in BAD-deficient mice, neonatal hypoxia-ischemia does not increase caspase-3 immunostaining compared with similarly treated wild-type animals (Ness et al., 2006), supporting the idea that BAD participates in the hypoxia-ischemia-induced apoptosis.

BCL-2 is implicated in survival and cell differentiation (see Cory et al., 2003). In the present study, BCL-2 levels increased in whole hippocampal extracts following perinatal asphyxia, perhaps restricting the progression of apoptosis. However, the BAD/BCL-2 ratio increased, indicating that an apoptotic mechanism prevailed and that the increase of BCL-2 was not enough to prevent cell death.

It has been reported that hypoxia-ischemia induces a biphasic increase of BCL-2 immunoreactivity in CA1, with peaks at P3 and P20, suggesting that BCL-2 is associated with both early and delayed neuroprotection (Daval et al., 2004). An increase of BCL-2 expression has also been observed in CA3 and DG after hypoxia-ischemia in adult rats (Chen et al., 1996). However, a down-regulation of BCL-2 transcription has been observed after left carotid artery occlusion followed by 2.5 hr of hypoxia exposure at P7 in rats (Kumral et al., 2006). Together, these results suggest that changes in BCL-2 expression probably depend on the severity of the insult and the developmental stage of the brain when the insult takes place.

Neurotrophic factors regulate BCL-2 expression through transcription factors, such as the cAMP response element binding (CREB) protein (Jin et al., 2001; see Lonze and Ginty, 2002; Lee et al., 2004) and nuclear factor-κB (NFκB; Tamatani et al., 1999, 2000). CREB activity is regulated through phosphorylation at Ser133 (P-CREB) by the ERK/MAPK pathway (Curtis and Finkbeiner, 1999). An increase of P-CREB levels has been observed 6 hr after ischemic insults (Walton et al., 1996; Lee et al., 2004). In the present study, however, no changes were detected in total CREB or its phosphorylated form 1 week after perinatal asphyxia, perhaps suggesting that the increase of BCL-2 by perinatal asphyxia was due to an early transient increase of CREB. Alternatively, BCL-2 gene expression can be regulated by NFκB, as reported by Tamatani et al. (1999, 2000), although in this study we did not monitored that factor.

In adults, new neurons can be generated in the subventricular zone (SVZ). The cells generated in SVZ migrate to the olfactory bulb (Doetsch et al., 1999; Shapiro et al., 2006), where they differentiate to interneurons (Doetsch et al., 1999). The rate of neurogenesis can be increased by brain injuries, including hypoxia-ischemia, probably corresponding to a compensatory mechanism for the replacement of dead cells (see Lichtenwalner and Parent, 2006). Neurogenesis in SVZ has been proposed also to contribute to neuronal replacement in the CA1 region after hypoxia-ischemia (Nakatomi et al., 2002; Ong et al., 2005). In agreement, we found here that perinatal asphyxia induced a twofold increase of BrdU-positive cells in the CA1 region, compared with control animals, but only 10% of those BrdU-positive cells were positive for MAP-2. No BrdU-positive cells were positive for MAP-2 in any of the regions of the cornu ammonis of control animals.

Cell proliferation has also been observed in SGZ of DG following hypoxia-ischemia (Scheepens et al., 2003b; Bartley et al., 2005). In agreement, it was found here that the number of BrdU positive cells was increased in the supra- and infrapyramidal band of DG and in hilus by perinatal asphyxia at P7. At P30, however, there was an increase only in the suprapyramidal band of the DG. This finding is in agreement with findings reported by Choi et al. (2003), showing an increase of cell proliferation in both supra- and infrapyramidal bands after 10 days but only in the medial suprapyramidal band after 28 days of global ischemia.

Double staining revealed that the number of BrdU/MAP-2-positive cells was increased in the supra- and infrapyramidal band of DG and in hilus by perinatal asphyxia, which is in agreement with a previous study with hippocampal organotypic cultures (Morales et al., 2005, 2007). In contrast to the CA1 region, ~40% of the total number of BrdU-positive cells were also positive for MAP-2 in DG, and the percentage of double-labelled cells was similar in both control and asphyxia-exposed animals. The remaining amount perhaps represented proliferation of progenitor cells, or cells at an earlier stage of differentiation, which can potentially differentiate to neurons (Ganat et al., 2002; Bartley et al., 2005) or to glial cells (Kee et al., 2001; Zaidi et al., 2004).

ERK1/2 proteins are associated with cell proliferation (Zhou et al., 2004) and have been found to be activated early (0–72 hr) after neonatal hypoxia/ischemia in hippocampus (Wang et al., 2003; Haddad, 2004; Jones and Bergeron, 2004). Interestingly, it has been reported that the activation of ERK1/2 proteins is inhibited by U0126, an inhibitor of mitogen-activated protein kinase (Favata et al., 1998), reducing the effect of hypoxia-ischemia on BrdU labelling (Zhou et al., 2004).

ERK activity is regulated through phosphorylation at threonine and tyrosine residues by the MAPK pathway (Boulton et al., 1991; see Haddad, 2004). In the present study, we found an increase of P-ERK2, but not of total ERK or P-ERK1, levels after the perinatal insult. It can be suggested that ERK2 phosphorylation is related to neurogenesis, but we cannot discard its participation in cell death in the perinatal asphyxia model, as suggested by Castro-Obregón et al. (2004). Indeed, it has been suggested that nuclear translocation of ERK2 is required for cell cycle progression (Hulleman et al., 1999; Chu et al., 2004).

The MEK/ERK pathway promotes CREB activation through phosphorylation (see Lonze and Ginty, 2002), increasing proliferation and cell differentiation in DG of adult mouse hippocampus (Nakagawa et al., 2002; Fujioka et al., 2004). In agreement, cell prolifera-

tion decreases in conditional transgenic mice expressing a CREB dominant negative mutant in hippocampus (Nakagawa et al., 2002). In the present study, no correlation between ERK activation and CREB phosphorylation was observed, but a transient early CREB activation could have taken place at earlier stages that was undetectable at P7.

bFGF is essential for neuronal development (Dono, 2003); it is involved in proliferation (Raballo et al., 2000) and differentiation (Vicario-Abejón et al., 1995; Cheng et al., 2002). The expression of bFGF is increased after brain injury (Takami et al., 1992; Andersson et al., 1995), promoting neurogenesis and survival (Wagner et al., 1999; Yoshimura et al., 2001). In the present study, there was an increase of bFGF expression in CA1, CA2, and hilus and bFGF levels in whole hippocampus 1 week and 1 month after perinatal asphyxia. Similar results have been observed following ischemia (Takami et al., 1992) and hypoxia (Ganat et al., 2002) in adult animals. It has been shown that intraventricular infusion of bFGF markedly augmented endogenous progenitor proliferation, leading to regeneration of CA1 neurons, ameliorating the neurological deficits induced by ischemia (Nakatomi et al., 2002). Overexpression of bFGF by a herpes simplex virus-1 vector increased significantly the number of dividing cells in DG, attenuating the effect of ischemia on cell death (Yoshimura et al., 2001). These results support the idea that bFGF up-regulates neurogenesis and protects neurons against degeneration of hippocampus, as shown after brain traumatic insults in adult animals (Yoshimura et al., 2001, 2003). Interestingly, it has been shown that both ERK1 and ERK2 are activated by bFGF (Hetman et al., 1999), suggesting that bFGF can induce the phosphorylation of ERK2, promoting cell proliferation, as reported here.

In conclusion, perinatal asphyxia induces regionally specific delayed cell death and neurogenesis in rat hippocampus accompanied by an increase of pro- and antiapoptotic proteins. The increased neurogenesis found in CA1, DG, and hilus of asphyxia-exposed animals together with the increased expression of mitogenic proteins suggest that plastic changes occur, perhaps providing a framework for functional recovery of the hippocampus.

ACKNOWLEDGMENTS

We are grateful for the excellent technical and secretarial help from Mr. Juan Santibañez, Ms. Carmen Almeyda, and Ms. Ana María Méndez. The support from the confocal unit (CESAT, ICBM), led by Dr. Jorge Sans, is kindly acknowledged.

REFERENCES

Abe T, Takagi N, Nakano M, Furuya M, Takeo S. 2004. Altered Bad localization and interaction between Bad and Bcl-x_L in the hippocampus after transient global ischemia. Brain Res 1009:159–168.

Amaral DG, Dent JA. 1981. Development of the mossy fibers of the dentate gyrus: I. A light and electron microscopic study of the mossy fibers and their expansions. J Comp Neurol 195:51–86.

Amaral DG, Witter MP. 1995. Hippocampal formation. In: Paxinos G, editor. The rat nervous system. San Diego: Academic Press.

Andersson K, Bjelke B, Bolme P, Ögren SO. 1992. Asphyxia-induced lesion of the rat hippocampus (CA1, CA3) and the nigro-striatal dopamine system. Hypoxia and ischemia. CNS. In: Gross J, editor. Wissenschaflige publikationen de Humboldt-Universität zu Berlin. B Medizin 41:71–76.

Andersson K, Blum M, Chen Y, Eneroth P, Gross J, Herrera-Marschitz M, Bjelke B, Bolme P, Diaz R, Jamison L, Loidl F, Ungethüm U, Åström G, Ögren SÖ. 1995. Perinatal asphyxia increases bFGF mRNA levels and DA cell body number in mesencephalon of rats. Neuroreport 6:375–337.

Andrés S, Cárdenas S, Parra C, Bravo J, Greiner M, Rojas P, Morales P, Lara H, Fiedler JL. 2006. Effect of long-term adrenalectomy on the apoptosis in rat hippocampus. Endocrine 29:299–307.

Aspberg A, Tottmar O. 1992. Development of antioxidant enzymes in rat brain and in reaggregation culture of fetal brain cells. Brain Res Dev Brain Res 66:55–58.

Bartley J, Soltau T, Wimborne H, Kim S, Martin-Studdard A, Hess D, Hill W, Waller J, Carroll J. 2005. BrdU-positive cells in the neonatal mouse hippocampus following hypoxic-ischemic brain injury. BMC Neurosci 6:15.

Bayer SA. 1982. Changes in the total number of dentate granule cells in juvenile and adult rats: a correlated volumetric and ^{3}H-thymidine autoradiographic study. Exp Brain Res 46:315–323.

Bjelke B, Andersson K, Ögren SO, Bolme P. 1991. Asphyctic lesion: proliferation of tyrosine hydroxylase-immunoreactive nerve cell bodies in the rat substantia nigra and functional changes in dopamine neurotransmission. Brain Res 543:1–9.

Boulton TG, Nye SH, Robbins DJ, Ip NY, Radziejewska E, Morgenbesser SD, DePinho RA, Panayotatos N, Cobb MH, Yancopoulos GD. 1991. ERKs: a family of protein-serine/threonine kinases that are activated and tyrosine phosphorylated in response to insulin and NGF. Cell 65:663–675.

Bradford MM. 1976. A rapid and sensitive method for the quantitation of microgram quantities of protein utilizing the principle of protein-dye binding. Anal Biochem 72:248–254.

Bustamante D, Morales P, Pereyra JT, Goiny M, Herrera-Marschitz M. 2006. Nicotinamide prevents the effect of perinatal asphyxia on dopamine release evaluated with in vivo microdialysis 3 months after birth. Exp Brain Res 177:358–369.

Cárdenas SP, Parra C, Bravo J, Morales P, Lara HE, Herrera-Marschitz M, Fiedler JL. 2002. Corticosterone differentially regulates bax, bcl-2 and bcl-x mRNA levels in the rat hippocampus. Neurosci Lett 331:9–12.

Castro-Obregon S, Rao RV, del Rio G, Chen SF, Poksay KS, Rabizadeh S, Vesce S, Zhang XK, Swanson RA, Bredesen DE. 2004. Alternative, nonapoptotic programmed cell death: mediation by arrestin 2, ERK2, and Nur77. J Biol Chem 279:17543–17553.

Chen J, Zhu RL, Nakayama M, Kawaguchi K, Jin K, Stetler RA, Simon RP, Graham SH. 1996. Expression of the apoptosis-effector gene, Bax, is up-regulated in vulnerable hippocampal CA1 neurons following global ischemia. J Neurochem 67:64–71.

Chen J, Nagayama T, Jin K, Stettler RA, Zhu RL, Graham SH, Simon RP. 1998. Induction of caspase-3-like protease may mediate delayed neuronal death in the hippocampus after transient cerebral ischemia. J Neurosci 18:4914–4928.

Chen Z, Kontonotas D, Friedmann D, Pitts-Kiefer A, Frederick JR, Siman R, Neumar RW. 2005. Developmental status of neurons selectively vulnerable to rapidly triggered post-ischemic caspase activation. Neurosci Lett 376:166–170.

Cheng Y, Gidday JM, Yan Q, Shah AR, Holtzman DM. 1997. Marked age-dependent neuroprotection by brain-derived neurotrophic against neonatal hypoxic-ischemic brain injury. Ann Neurol 41:521–529.

Cheng Y, Deshmukh M, D'Costa A, Demaro JA, Gidday JM, Shah A, Sun Y, Jacquin MF, Johnson EM, Holtzman DM. 1998. Caspase inhibitor affords neuroprotection with delayed administration in a rat model of neonatal hypoxic-ischemic brain injury. J Clin Invest 101:1992–1999.

Cheng Y, Black IB, DiCicco-Bloom E. 2002. Hippocampal granule neuron production and population size are regulated by levels of bFGF. Eur J Neurosci 15:3–12.

Choi YS, Lee MY, Sung KW, Jeong SW, Choi JS, Park HJ, Kim ON, Lee SB, Kim SY. 2003. Regional differences in enhanced neurogenesis in the dentate gyrus of the adult rats after transient forebrain ischemia. Mol Cells 16:232–238.

Chu CT, Levinthal DJ, Kulich SM, Chalovich EM, DeFranco DB. 2004. Oxidative neuronal injury. The dark side of ERK1/2. Eur J Biochem 271:2060–2066.

Cory S, Huang DC, Adams JM. 2003. The Bcl-2 family: roles in cell survival and oncogenesis. Oncogene 22:8590–8607.

Curtis J, Finkbeiner S. 1999. Sending signals from the synapse to the nucleus: possible roles for CaMK, Ras/ERK, and SAPK pathways in the regulation of synaptic plasticity and neuronal growth. J Neurosci Res 58:88–95.

Daval JL, Pourie G, Grojean S, Lievre V, Strazielle G, Vert P. 2004. Neonatal hypoxia triggers transient apoptosis followed by neurogenesis in the rat CA1 hippocampus. Pediatric Res 55:561–567.

Davies JC. 1995. The Bcl-2 family of proteins, and the regulation of cell survival. Trends Neurol Sci 18:355–358.

Dell'Anna E, Chen Y, Engidawork E, Andersson K, Lubec G, Luthman J, Herrera-Marschitz M. 1997. Delayed neuronal death following perinatal asphyxia in rat. Exp Brain Res 115:105–115.

Dluzniewska J, Beresewicz M, Wojewodzka U, Gajkowska B, Zablocka B. 2005. Transient cerebral ischemia induces delayed proapoptotic Bad translocation to mitochondria in CA1 sector of hippocampus. Brain Res Mol Brain Res 133:274–280.

Doetsch F, Caille I, Lim DA, Garcia-Verdugo JM, Alvarez-Buylla A. 1999. Subventricular zone astrocytes are neural stem cells in the adult mammalian brain. Cell 97:703–716.

Dono R. 2003. Fibroblast growth factors as regulators of central nervous system development and function. Am J Physiol Regul Integr Comp Physiol 284:R867–R881.

Favata MF, Horiuchi KY, Manos EJ, Daulerio AJ, Stradley DA, Feeser WS, Van Dyk DE, Pitts WJ, Earl RA, Hobbs F, Copeland RA, Magolda RL, Scherle PA, Trzaskos JM. 1998. Identification of a novel inhibitor of mitogen-activated protein kinase kinase. J Biol Chem 273:18623–18632.

Ferrer I, Pozas E, López E, Ballabriga J. 1997. Bcl-2, Bax and Bcl-x expression following hypoxia-ischemia in the infant rat brain. Acta Neuropathol 94:583–589.

Fujioka T, Fujioka A, Duman RS. 2004. Activation of cAMP signaling facilitates the morphological maturation of newborn neurons in adult hippocampus. J Neurosci 24:319–328.

Ganat Y, Soni S, Chacon M, Schwartz ML, Vaccarino FM. 2002. Chronic hypoxia up-regulates fibroblast growth factor ligands in the perinatal brain and induces fibroblast growth factor-responsive radial glial cells in the subependymal zone. Neuroscience 112:977–991.

Golan H, Huleihel M. 2006. The effect of prenatal hypoxia on brain development: short- and long-term consequences demonstrated in rodent models. Dev Sci 9:338–349.

Graham EM, Sheldon RA, Flock DL, Ferriero DM, Martin LJ, O'Riordan DP, Northington FJ. 2004. Neonatal mice lacking functional Fas death receptors are resistant to hypoxic-ischemic brain injury. Neurobiol Dis 17:89–98.

Greiner M, Cárdenas S, Parra C, Bravo J, Avalos AM, Paredes A, Lara HE, Fiedler JL. 2001. Adrenalectomy regulates apoptotic-associated genes in rat hippocampus. Endocrine 15:323–333.

Gundersen NJ, Bagger P, Bendtsen TF, Evans SM, Korbo L, Marcussen H, Møller A, Nielsen K, Nyengaard JR, Pakkenberg B, Sørensen FB, Vesterby A, West MJ. 1988. The new stereological tools: disector, fractionator, nucleator and point sampled interecepts and their use in pathologic research and diagnosis. Acta Pathol Microbial Immunol Scand 96:857–881.

Haddad JJ. 2004. Hypoxia and the regulation of mitogen-activated protein kinases: gene transcription and the assessment of potential pharmacologic therapeutic interventions. Int Immunopharmacol 4:1249–1285.

Han BH, Holtzman DM. 2000. BDNF protects the neonatal brain from hypoxic-ischemic injury in vivo via the ERK pathway. J Neurosci 20:5775–5781.

Harry JG, d'Hellencourt CL. 2003. Dentate gyrus: alterations that occur with hippocampal injury. Neurotoxicology 24:343–356.

Herrera-Marschitz M, Loidl CF, Andersson K, Ungerstedt U. 1993. Prevention of mortality induced by perinatal asphyxia: hypothermia or glutamate antagonism? Amino Acids 5:413–419.

Hetman M, Kanning K, Cavanaugh JE, Xia Z. 1999. Neuroprotection by brain-derived neurotrophic factor is mediated by extracellular signal-regulated kinase and phosphatidylinositol 3-kinase. J Biol Chem 274:22569–22580.

Hirai K, Hayashi T, Chan PH, Zeng J, Yang GY, Basus VJ, James TL, Litt L. 2004. PI3K inhibition in neonatal rat brain slices during and after hypoxia reduces phospho-Akt and increases cytosolic cytochrome c and apoptosis. Brain Res Mol Brain Res 124:51–61.

Howard S, Bottino C, Brooke S, Cheng E, Giffard RG, Sapolsky R. 2002. Neuroprotective effects of bcl-2 overexpression in hippocampal cultures: interactions with pathways of oxidative damage. J Neurochem 83:914–923.

Hulleman E, Bijvelt JJ, Verkleij AJ, Verrips CT, Boonstra J. 1999. Nuclear translocation of mitogen-activated protein kinase p42MAPK during the ongoing cell cycle. J Cell Physiol 180:325–333.

Jin K, Mao XO, Simon RP, Greenberg DA. 2001. Cyclic AMP response element binding protein (CREB) and CREB binding protein (CBP) in global cerebral ischemia. J Mol Neurosci 16:49–56.

Jin K, Mao XO, Zhu Y, Greenberg DA. 2002. MEK and ERK protect hypoxic cortical neurons via phosphorylation of Bad. J Neurochem 80:119–125.

Jones NM, Bergeron M. 2004. Hypoxia-induced ischemic tolerance in neonatal rat brain involves enhanced ERK1/2 signalling. J Neurochem 89:157–167.

Kee NJ, Preston E, Wojtowicz JM. 2001. Enhanced neurogenesis after transient global ischemia in the dentate gyrus of the rat. Exp Brain Res 136:313–320.

Kirino T, Tamura A, Sano K. 1984. Delayed death in the rat hippocampus following transient forebrain ischemia. Acta Neuropathol 64:139–147.

Kobayashi T, Ahlenius H, Thored P, Kobayashi R, Kokaia Z, Lindvall O. 2006. Intracerebral infusion of glial cell line-derived neurotrophic factor promotes striatal neurogenesis after stroke in adult rats. Stroke 37:2361–2367.

Kumral A, Genc S, Ozer E, Yilmaz O, Gokmen N, Koroglu TF, Duman N, Genc K, Ozkan H. 2006. Erythropoietin downregulates bax and DP5 proapoptotic gene expression in neonatal hypoxic-ischemic brain injury. Biol Neonate 89:205–210.

Lafemina MJ, Sheldon RA, Ferriero DM. 2006. Acute hypoxia-ischemia results in hydrogen peroxide accumulation in neonatal but not adult mouse brain. Pediatric Res 59:680–683.

Lee HT, Chang YC, Wang LY, Wang ST, Huang CC, Ho CJ. 2004. cAMP response element-binding protein activation in ligation preconditioning in neonatal brain. Ann Neurol 56:611–623.

Li LY, Luo X, Wang X. 2001. Endonuclease G is an apoptotic DNase when released from mitochondria. Nature 412:95–99.

Lichtenwalner RJ, Parent JM. 2006. Adult neurogenesis and the ischemic forebrain. J Cereb Blood Flow Metab 26:1–20.

Lipton P. 1999. Ischemic cell death in brain neurons. Physiol Rev 79:1431–1540.

Lonze BE, Ginty DD. 2002. Function and regulation of CREB family transcription factors in the nervous system. Neuron 35:605–623.

Matsumori Y, Hong SM, Aoyama K, Fan Y, Kayama T, Sheldon RA, Vexler ZS, Ferriero DM, Weinstein PR, Liu J. 2005. Hsp70 overexpression sequesters AIF and reduces neonatal hypoxic/ischemic brain injury. J Cereb Blood Flow Metab 25:899–910.

Morales P, Reyes P, Klawitter V, Huaiquín P, Bustamante D, Fiedler JL, Herrera-Marschitz M. 2005. Effects of perinatal asphyxia on cell proliferation and neuronal phenotype evaluated with organotypic hippocampal cultures. Neuroscience 135:421–431.

Morales P, Huaiquin P, Bustamante D, Fiedler J, Herrera-Marschitz M. 2007. Perinatal asphyxia induces neurogenesis in hippocampus: an organotypic culture study. Neurotoxicity Res 12:81–84.

Nakagawa S, Kim JE, Lee R, Malberg JE, Chen J, Steffen C, Zhang YJ, Nestler EJ, Duman RS. 2002. Regulation of neurogenesis in adult mouse hippocampus by cAMP and the cAMP response element-binding protein. J Neurosci 22:3673–3682.

Nakajima W, Ishida A, Lange MS, Gabrielson KL, Wilson MA, Martin LJ, Blue ME, Johnston MV. 2000. Apoptosis has a prolonged role in the neurodegeneration after hypoxic ischemia in the newborn rat. J Neurosci 20:7994–8004.

Nakano S, Kogure K, Fujikura H. 1990. Ischemia-induced slowly progressive neuronal damage in the rat brain. Neuroscience 38:115–124.

Nakatomi H, Kuriu T, Okabe S, Yamamoto S, Hatano O, Kawahara N, Tamura A, Kirino T, Nakafuku M. 2002. Regeneration of hippocampal pyramidal neurons after ischemic brain injury by recruitment of endogenous neural progenitors. Cell 110:429–441.

Ness JM, Harvey CA, Strasser A, Bouillet P, Klocke BJ, Roth KA. 2006. Selective involvement of BH3-only Bcl-2 family members Bim and Bad in neonatal hypoxia-ischemia. Brain Res 1099:150–159.

Northington FJ, Ferriero DM, Graham EM, Traystman RJ, Martin LJ. 2001. Early neurodegeneration after hypoxia-ischemia in neonatal rat is necrosis while delayed neuronal death is apoptosis. Neurobiol Dis 8:207–219.

Ong J, Plane JM, Parent JM, Silverstein FS. 2005. Hypoxic-ischemic injury stimulates subventricular zone proliferation and neurogenesis in the neonatal rat. Pediatric Res 58:600–606.

Oppenheim RW. 1991. Cell death during development of the nervous system. Annu Rev Neurosci 14:453–501.

Paxinos G, Watson C. 1986. The rat brain in stereotaxic coordinates. New York: Academic Press.

Pourie G, Blaise S, Trabalon M, Nedelec E, Gueant JL, Daval JL. 2006. Mild, non-lesioning transient hypoxia in the newborn rat induces delayed brain neurogenesis associated with improved memory scores. Neuroscience 140:1369–1379.

Pulsinelli WA. 1988. Selective neuronal vulnerability: morphological and molecular characteristics. Prog Brain Res 63:29–37.

Raballo R, Rhee J, Lyn-Cook R, Leckman JF, Schwartz ML, Vaccarino FM. 2000. Basic fibroblast growth factor (Fgf2) is necessary for cell proliferation and neurogenesis in the developing cerebral cortex. J Neurosci 20:5012–5023.

Scheepens A, Wassink G, Blanco CE. 2003a. The effect of a global birth asphyxia on the ontogeny of BDNF and NGF protein expression in the juvenile brain. Brain Res Dev Brain Res 140:215–221.

Scheepens A, Wassink G, Piersma MJ, Van de Berg WDJ, Blanco CE. 2003b. A delayed increase in hippocampal proliferation following global asphyxia in the neonatal rat. Brain Res Dev Brain Res 142:67–76.

Shapiro EM, Gonzalez-Perez O, Manuel Garcia-Verdugo J, Alvarez-Buylla A, Koretsky AP. 2006. Magnetic resonance imaging of the migration of neuronal precursors generated in the adult rodent brain. Neuroimage 32:1150–1157.

Shimasaki S, Emoto N, Koba A, Mercado M, Shibata F, Cooksey K, Baird A, Ling N. 1988. Complementary DNA cloning and sequencing of rat ovarian basic fibroblast growth factor and tissue distribution study of its mRNA. Biochem Biophys Res Commun 157:256–263.

Takami K, Iwane M, Kiyota Y, Miyamoto M, Tsukuda R, Shiosaka S. 1992. Increase of basic fibroblast growth factor immunoreactivity and its mRNA level in rat brain following transient forebrain ischemia. Exp Brain Res 90:1–10.

Tamatani M, Che YH, Matsuzaki H, Ogawa S, Okado H, Miyake S, Mizuno T, Tohyama M. 1999. Tumor necrosis factor induces Bcl-2 and Bcl-x expression through NFkappaB activation in primary hippocampal neurons. J Biol Chem 274:8531–8538.

Tamatani M, Mitsuda N, Matsuzaki H, Okado H, Miyake SI, Vitek MP, Yamaguchi A, Tohyama M. 2000. A pathway of neuronal apoptosis induced by hypoxia/reoxygenation: roles of nuclear factor-κB and Bcl-2. J Neurochem 75:683–693.

Tan Y, Demeter MR, Ruan H, Comb MJ. 2000. BAD Ser-155 phosphorylation regulates BAD/Bcl-xL interaction and cell survival. J Biol Chem 275:25865–25869.

Van Erp TGM, Saleh PA, Rosso PA, Huttunen M, Lönnqvist J, Pirkola T, Salonen O, Valanne L, Poutanen V-P, Standersköld-Nordenstam C-G, Cannon TD. 2002. Contributions of genetic risk and fetal hypoxia to hippocampal volume in patients with schizophrenia or schizoaffective disorder, their unaffected siblings and healthy unrelated volunteers. Am J Psychiatry 159:1514–1520.

Vannucci SJ, Hagberg H. 2004. Hypoxia-ischemia in the immature brain. J Exp Biol 207:3149–3154.

Vicario-Abejon C, Johe KK, Hazel TG, Collazo D, McKay RD. 1995. Functions of basic fibroblast growth factor and neurotrophins in the differentiation of hippocampal neurons. Neuron 15:105–114.

Wagner JP, Black IB, DiCicco-Bloom E. 1999. Stimulation of neonatal and adult brain neurogenesis by subcutaneous injection of basic fibroblast growth factor. J Neurosci 19:6006–6016.

Walton M, Sirimanne E, Williams C, Gluckman P, Dragunow M. 1996. The role of the cyclic AMP-responsive element binding protein (CREB) in hypoxic-ischemic brain damage and repair. Brain Res Mol Brain Res 43:21–29.

Wang HD, Fukuda T, Suzuki T, Hashimoto K, Liou SY, Momoi T, Kosaka T, Yamamoto K, Nakanishi H. 1999a. Differential effects of Bcl-2 overexpression on hippocampal CA1 neurons and dentate granule cells following hypoxic ischemia in adult mice. J Neurosci Res 57:1–12.

Wang HG, Pathan N, Ethell IM, Krajewski S, Yamaguchi Y, Shibasaki F, McKeon F, Bobo T, Franke TF, Reed JC. 1999b. Ca^{2+}-induced apoptosis through calcineurin dephosphorylation of BAD. Science 284:339–343.

Wang X, Zhu C, Qiu L, Hagberg H, Sandberg M, Blomgren K. 2003. Activation of ERK1/2 after neonatal rat cerebral hypoxia-ischaemia. J Neurochem 86:351–362.

Weitzdoerfer R, Pollak A, Lubec B. 2004. Perinatal asphyxia in the rat has lifelong effects on morphology, cognitive functions, and behavior. Semin Perinatol 28:249–256.

Yagita Y, Kitagawa K, Ohtsuki T, Takasawa K, Miyata T, Okano H, Hori M, Matsumoto M. 2001. Neurogenesis by progenitor cells in the ischemic adult rat hippocampus. Stroke 32:1890–1896.

Yang E, Zha J, Jockel J, Boise LH, Thompson CB, Korsmeyer SJ. 1995. Bad, a heterodimeric partner for Bcl-xL and Bcl-2, displaces Bax and promotes cell death. Cell 80:285–291.

Yoshimura S, Takagi Y, Harada J, Teramoto T, Thomas SS, Waeber C, Bakowska JC, Breakefield XO, Moskowitz MA. 2001. FGF-2 regulation of neurogenesis in adult hippocampus after brain injury. Proc Natl Acad Sci U S A 98:5874–5879.

Yoshimura S, Teramoto T, Whalen MJ, Irizarry MC, Takagi Y, Qiu J, Harada J, Waeber C, Breakefield XO, Moskowitz MA. 2003. FGF-2 regulates neurogenesis and degeneration in the dentate gyrus after traumatic brain injury in mice. J Clin Invest 112:1202–1210.

Yuan J, Yankner ,BA. 2000. Apoptosis in the nervous system. Nature 407:802–809.

Zaidi AU, Bessert DA, Ong JE, Xu H, Barks JD, Silverstein FS, Skoff RP. 2004. New oligodendrocytes are generated after neonatal hypoxic-ischemic brain injury in rodents. Glia 46:380–930.

Zha J, Harada H, Yang E, Jockel J, Korsmeyer SJ. 1996. Serine phosphorylation of death agonist BAD in response to survival factor results in binding to 14-3-3 not BCL-X_L. Cell 87:619–628.

Zhou L, Del Villar K, Dong Z, Miller CA. 2004. Neurogenesis response to hypoxia-induced cell death: map kinase signal transduction mechanisms. Brain Res 1021:8–19.

Zhu C, Qiu L, Wang X, Hallin U, Cande C, Kroemer G, Hagberg H, Blomgren K. 2003. Involvement of apoptosis-inducing factor in neuronal death after hypoxia-ischemia in the neonatal rat brain. J Neurochem 86:306–317.

Zhu C, Xu F, Wang X, Shibata M, Uchiyama Y, Blomgren K, Hagberg H. 2006. Different apoptotic mechanisms are activated in male and female brains after neonatal hypoxia-ischaemia. J Neurochem 96:1016–1027.

Zhu Y, Yang GY, Ahlemeyer B, Pang L, Che XM, Culmsee C, Klumpp S, Krieglstein J. 2002. Transforming growth factor-beta 1 increases bad phosphorylation and protects neurons against damage. J Neurosci 22:3898–3909.